1220
doi:10.1017/S1431927622005086
Microsc. Microanal. 28 (Suppl 1), 2022

Second-order Total Variation for Compressed Sensing Cryo-ET and Subtomogram Averaging

Jan Böhning,[1] Tanmay A.M. Bharat,[1,2] and Sean M. Collins,[3*]

[1.] Sir William Dunn School of Pathology, University of Oxford, Oxford, UK.
[2.] Structural Studies Division, MRC Laboratory of Molecular Biology, Cambridge, UK.
[3.] School of Chemical and Process Engineering & School of Chemistry, University of Leeds, Leeds, UK.
* Corresponding author: s.m.collins@leeds.ac.uk

Cryo-electron tomography (cryo-ET) is a key tool for imaging macromolecules in cellular environments. Together with subtomogram averaging (STA), cryo-ET can be used for structure determination. Weak visibility of many structures in cryo-ET as well as the volume of data required for STA, however, motivate the exploration of advanced image processing for cryo-ET. Compressed sensing is a mathematically rigorous signal processing approach to sampling with far fewer measurements than traditionally required, with significant applications in limited angle, undersampled electron tomography in the physical sciences [1,2]. Compressed sensing electron tomography (CS-ET) holds that for sample features that can be described as sparse, i.e., those requiring only a few coefficients to represent the object in a particular mathematical transform domain, a set of measurements can be devised to directly identify the tomographic reconstruction that also adheres to that sparsity, in contrast to post-processing approaches. This idea is related to image compression, where an image can be represented by only a small number of coefficients to reduce the storage requirements of the fully sampled image. CS-ET enables reducing data quantities while recovering high-fidelity reconstructions, or provides improved visibility and precision of image features for a given number of samples (measurements) [1–3].

Identifying suitable and general sparse domains for cryo-ET and determining whether these preserve high-resolution structural information is essential. CS-ET has seen several applications in cryo-ET to date [4,5], but high-resolution structures have not been reported. Moreover, advances in CS-ET, including the use of higher order total variation and three-dimensional transforms matched to the three-dimensional object under reconstruction, have not been assessed for cryo-ET. Second-order total variation (CS-TV^2) has recently seen wider application in physical sciences CS-ET [6]. Whereas first-order total variation reinforces tomographic reconstructions that are piece-wise constant, structures of interest in cryo-ET exhibit intensity variations with relatively high image density in high-resolution structures, limiting the applicability of sparsity in the image of an object itself. CS-TV^2 allows for variation in intensity while reinforcing the inherent connectivity of structures in three-dimensions.

To evaluate CS-TV^2, we first evaluated whether the reconstruction algorithm retains information to the secondary structure level in hepatitis B (HBV) triangulation number (T) = 4 capsid particles [7]. Fig. 1 shows a comparison of WBP and CS-TV^2 reconstructions, confirming CS-TV^2 enhances visibility of structures with small fractions of the full dataset and preserves information at the secondary structure level. Application of CS-TV^2 to *C. crescentus* cells demonstrated that the approach shows wider utility (Fig. 2). In cellular specimens, in particular, the visibility of features is significantly improved in CS-TV^2 relative to WBP reconstructions. This presentation will discuss important data pre-processing steps, selection of parameters for the evaluated CS-TV^2 implementation [8], approaches to parallelization, and directions for further development [9].

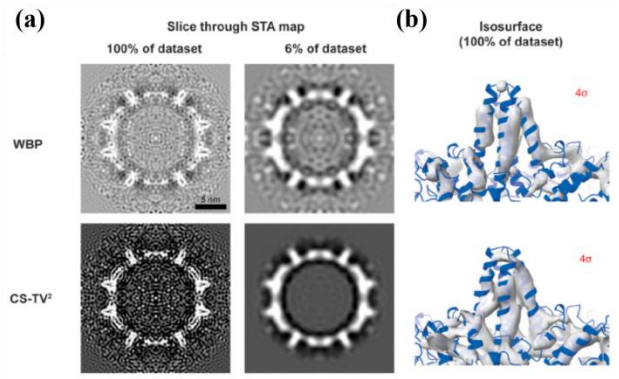

Figure 1. STA results from HBV capsid particles (188 particles at 100%, 12 particles at 6%) shown as (a) orthoslices and (b) isosurface renderings at 4σ isosurface contour level along with an atomic model (PDB: 6HTX) rigid body fitted into the density. Adapted from Ref. [7] (CC-BY).

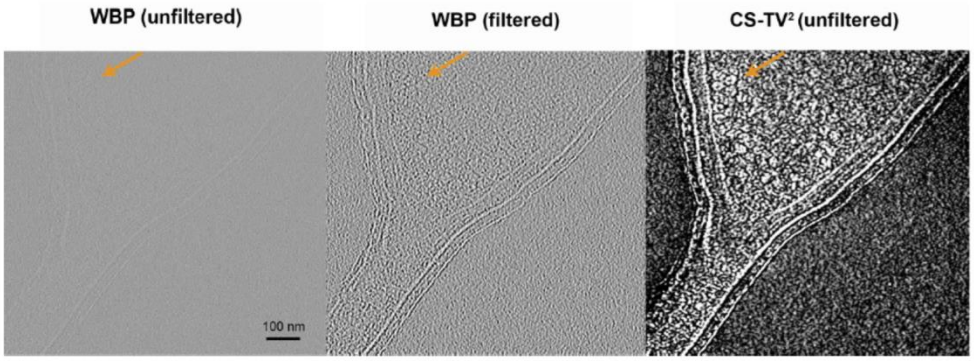

Figure 2. Orthoslices from reconstructions of a *C. crescentus* cell. Adapted from Ref. [7] (CC-BY).

References:
[1] Z. Saghi, D.J. Holland, R. Leary, A. Falqui, G. Bertoni, A.J. Sederman, L.F. Gladden, P.A. Midgley, Nano Lett. **11** (2011), p. 4666. https://doi.org/10.1021/nl202253a.
[2] R. Leary, Z. Saghi, P.A. Midgley, D.J. Holland, Ultramicroscopy **131** (2013), p. 70. https://doi.org/10.1016/j.ultramic.2013.03.019.
[3] Z. Saghi, G. Divitini, B. Winter, R. Leary, E. Spiecker, C. Ducati, P.A. Midgley, Ultramicroscopy **160** (2016), p. 230. https://doi.org/10.1016/j.ultramic.2015.10.021.
[4] M.D. Guay, W. Czaja, M.A. Aronova, R.D. Leapman, Sci. Rep. **6** (2016), 27614. https://doi.org/10.1038/srep27614.
[5] Y. Deng, Y. Chen, Y. Zhang, S. Wang, F. Zhang, F. Sun, J. Struct. Biol. **195** (2016), p. 100. https://doi.org/10.1016/j.jsb.2016.04.004.
[6] S.M. Collins, K.E. MacArthur, L. Longley, R. Tovey, M. Benning, C.-B. Schönlieb, T.D. Bennett, P.A. Midgley, APL Materials **7** (2019), 091111. https://doi.org/10.1063/1.5120093.
[7] J. Böhning, T.A.M. Bharat, S.M. Collins, Structure **30** (2022), p. 1. https://doi.org/10.1016/j.str.2021.12.010.
[8] R. Tovey, ToveyTomoTools, 2022. https://github.com/robtovey/ToveyTomoTools (accessed February 8, 2022).
[9] The authors acknowledge funding from the Wellcome Trust and the Royal Society (202231/Z/16/Z), the Vallee Research Foundation, the Leverhulme Trust, the John Fell Fund, the Medical Research Council (MR/K501256/1, MR/N013468/1), and ARC3 computing facilities (U. Leeds).

https://doi.org/10.1017/S1431927622005086 Published online by Cambridge University Press